

# Wildfire Altering Terrestrial Precursors of Disinfection Byproducts in Forest Detritus

Jun-Jian Wang,<sup>†</sup> Randy A. Dahlgren,<sup>‡</sup> Mahmut S. Erşan,<sup>§</sup> Tanju Karanfil,<sup>§</sup> and Alex T. Chow<sup>\*†</sup>

<sup>†</sup>Baruch Institute of Coastal Ecology and Forest Science, Clemson University, Georgetown, South Carolina 29442, United States

<sup>‡</sup>Department of Land, Air and Water Resources, University of California–Davis, Davis, California 95616, United States

<sup>§</sup>Department of Environmental Engineering and Earth Sciences, Clemson University, Anderson, South Carolina 29625, United States

## Supporting Information

**ABSTRACT:** Wildfire occurrence and intensity are increasing worldwide causing severe disturbances to forest watersheds used for potable water supply. The effects of wildfire on drinking water quality are not well understood, especially in terms of terrestrial dissolved organic matter (DOM) and DOM-associated formation of disinfection byproducts (DBP). As the forest floor layer is a major source of terrestrial DOM, we investigated characteristics and DBP formation of water extractable organic matter (WEOM) from the 0–5 cm depth of nonburned detritus (control) and burned detritus with black ash (moderate severity) and white ash (high severity) associated with the 2013 Rim Fire in California. Spectroscopic results suggested that the aromaticity of WEOM followed white ash > control > black ash and fluorescence region II (excitation 220–250 nm; emission 330–380 nm) of the emission-excitation-matrix was identified as a potential burn severity indicator. Compared to the control, WEOM from white and black ashes had lower reactivity in forming trihalomethanes (55%-of-control) and haloacetic acids (67%-of-control), but higher reactivity in forming the more carcinogenic haloacetonitrile after chlorination (244%-of-control) and *N*-nitrosodimethylamine after chloramination (229%-of-control). There was no change in reactivity for chloral hydrate formation, while WEOM from black ash showed a higher reactivity for haloketone formation (150%-of-control). Because wildfire consumed a large portion of organic matter from the detritus layer, there was lower water extractable organic carbon (27%-of-control) and organic nitrogen (19%-of-control) yields in ashes. Consequently, the wildfire caused an overall reduction in water extractable terrestrial DBP precursor yield from detritus materials.



## INTRODUCTION

Forest watersheds play an important role in water supply worldwide with approximately one-third of the USA population (>123 million) receiving drinking water sourced from forest watersheds.<sup>1</sup> One of the major threats to these drinking water supplies is wildfire, which globally burns 300 to 450 million hectares annually<sup>2</sup> and is expected to increase in intensity, size, and frequency given projections for future climate change.<sup>3</sup> For example, in the western USA, the average wildfire frequency, total area burned, and length of fire season during 1987–2003 increased by approximately 300%, 550%, and 60%, respectively, compared to the average from 1970 to 1986.<sup>3</sup> Depending on the wildfire extent and severity,<sup>4</sup> postfire deterioration in water quality (e.g., sediments and nutrient loads, organic and inorganic pollutants) may create additional challenges for water utilities to produce potable water.<sup>2,5</sup> Wildfire is expected to alter the characteristics of terrestrial dissolved organic matter (DOM) which plays an important role in pollutant fate and transport processes. Understanding how the quantity and quality of terrestrial DOM are altered by wildfire is therefore important to reveal linkages among forest disturbance, water quality, human health, and climate change.<sup>6</sup>

There is a paucity of information concerning the impact of wildfire on drinking water quality, especially regarding the formation of disinfection byproducts (DBPs) during water treatment.<sup>2,7</sup> DBPs are formed in reactions between oxidants (e.g., chlorine, chloramine, ozone) and organic (e.g., DOM) and inorganic (e.g., bromide) precursors in water.<sup>8–10</sup> DBP formation is unintended during bacteria/pathogen inactivation,<sup>11</sup> and this process strongly depends on disinfectant type and dose, precursor quantity and characteristics, and reaction conditions (e.g., pH and temperature).<sup>12</sup> Since the first report of DBPs in the 1970s, there has been an abundance of evidence linking human DBP exposure to bladder cancer, rectal cancer, adverse birth outcomes, and other health risks by dermal absorption, drinking, and inhalation.<sup>13</sup> Therefore, the Stage 2 disinfectants and disinfection byproducts rule of the U.S. EPA set an enforceable regulation of maximum contamination levels for trihalomethanes (THMs) and haloacetic acids (HAAs) at 80 and 60  $\mu\text{g/L}$ , respectively.<sup>14</sup> Although only 11 DBPs are

Received: December 1, 2014

Revised: April 11, 2015

Accepted: April 20, 2015

currently regulated in the USA, several others are formed during water treatment including nitrogenous DBPs [e.g., haloacetonitriles (HANs) and *N*-nitrosodimethylamine (NDMA)] which have been shown to be more cytotoxic and genotoxic than regulated carbonaceous DBPs.<sup>15</sup>

Previous research demonstrated that water quality was affected by intensive forest disturbance in the watershed, such as wildfire<sup>4</sup> and harvesting.<sup>16</sup> For example, drinking water quality was affected by changes in dissolved organic carbon (DOC) and DBP formation attributed to bark-beetle-caused tree mortality in the forest watershed.<sup>17</sup> Compared to such chronic change by forest die-off, wildfire causes a more intensive, acute, and long-term forest mortality that is recognized as one of the strongest natural disturbances.<sup>18</sup> The combustion losses of organic-rich soil horizons and vegetation biomass may reduce the amount of DOC exported from detritus materials. Furthermore, wildfire accelerates carbon and nitrogen mineralization and modifies the chemical composition of the detritus layer, converting lignin and polysaccharide rich and relatively degradable carbon pools to polycyclic aromatic, charcoal-rich, and recalcitrant black carbon.<sup>19,20</sup> Such an extreme change in the DOM source is expected to extensively alter DOM structure and its reactivity in forming DBPs. Recently, Writer et al.<sup>7</sup> studied water quality and DOM reactivity in forming DBPs after the High Park wildfire in Colorado and found no consistent differences in DOC level and DBP formation between burned and nonburned watersheds. However, <10% of the studied watershed was burned, and large differences in watershed characteristics and background autochthonous DOM between burned and nonburned watersheds may have concealed the actual effects of wildfire on terrestrial DOM chemistry and DBP formation. To minimize interferences from nonburned watershed areas and reveal the potential net impact of fire activity on characteristics of fire-affected terrestrial DOM and associated reactivity in DBP formation, we extracted DOM from burned and nonburned detritus for comparison in this study.

The Rim Fire in 2013, recorded as the third largest wildfire in California history, burned more than 100 000 ha in watersheds supplying drinking water for 2.6 million residences in/around San Francisco, CA. The wildfire converted organic matter stored in vegetation and the soil detritus layer to pyrogenic or incompletely burned materials ranging from black ash (moderate burning; commonly 200–500 °C) to white ash (severe burning; commonly >510 °C) (Figure S1, Supporting Information).<sup>21,22</sup> DOM leaching from these materials could enter source water supplies during rainfall events, affecting drinking water treatment and DBP formation in finished waters. To determine the impacts of wildfire on terrestrial DBP precursors in forest watersheds, we collected surface detritus materials (0–5 cm) from five burned sites within the Rim Fire perimeter (Figure S2, Supporting Information) and four nonburned sites outside the affected areas prior to any rainfall events. Water extracts from these materials along the burn severity gradient (nonburned → black ash → white ash) were characterized for general water quality, DOM quantity and quality, and DBP formation. The DBP formation was the focus, and we examined the formation of carbonaceous (e.g., THMs and HAAs), oxygenated (e.g., chloral hydrate (CHD) and haloketones (HKs)), and nitrogenous (e.g., HANs and NDMA) DBPs during chlorination or chloramination. To our knowledge, this is the first study to quantify the effects of wildfire on DBP formation potential from pure terrestrial DOM

originating from burned and nonburned detritus materials and to relate DOM reactivity to fire-induced changes in DOM characteristics.

## ■ MATERIALS AND METHODS

**Site Information and Soil Sampling.** Postfire soil samples (moderate severity vs high severity) were collected from 5 sites along a 13 km transect spanning the north–south axis of the Rim Fire (Figure S2 and Table S1, Supporting Information) in the Tuolumne River Watershed within the Stanislaus National Forest. This representative transect was selected to contain the most representative vegetation types in the burned area (ponderosa pine (site #1), mixed conifer forest (sites #2 and #3), mixed oak woodlands (site #4), and chaparral (site #5)). Ponderosa pine and white fir were present at all sites. Ash was characterized by color, which is one of the most visible and diagnostic features of fuel combustion completeness, or the burn severity.<sup>21</sup> On the basis of the visual characteristics of the ash, burn severity was classified as moderate severity characterized by complete consumption of the litter layer and formation of black ash (200–500 °C) or high severity with formation of white ash (>510 °C).<sup>22</sup>

Samples were collected on Oct 2, 2013 (fire ignition on Aug 17, 2013 and full containment on Oct 24, 2013) prior to rainfall events and thus represented nonleached materials. At each site, three composite samples of “white” and “black” ash samples were randomly collected along a 50 m transect using a 7.6 cm diameter × 5.0 cm depth metal coring device. The ash depth was generally 5 cm thick with the white ash samples somewhat thicker than the black ash samples. Each composite sample consisted of three subsamples collected within a 10 m radius. Detritus from nonburned sites (dominated by ponderosa pine or white fir) were collected from a forest located about 2 km north of the northern-most burned-area sampling site (site 1) near Cherry Lake (Table S1, Supporting Information).

There was complete mortality of vegetation and complete O horizon consumption at all five burned sites. Inspection of the remaining burned trees and shrubs allowed us to characterize the dominant woody vegetation assemblage at each site (Table S1, Supporting Information). Estimates of burn severity based on white vs black ash distribution were 8–10% high severity and 90–92% moderate severity at sites #2–5 and 3% high severity and 97% moderate severity at site #1.

**Dissolved Organic Matter Extraction.** All ash/detritus samples were air-dried at room temperature (22 ± 1 °C) until constant weight and passed through a 2 mm screen. The forest floor layer is a major source of terrestrial DOM.<sup>23</sup> To obtain the terrestrial DOM, we extracted the water extractable organic matter (WEOM) from ash/detritus material by mixing 40.0 g of ash/detritus sample with 200 mL of Milli-Q water in a 250 mL Erlenmeyer flask for 2 h. The supernatant was filtered through a pre-rinsed 0.45 μm polyethersulfone filter and stored at 4 °C before further analyses.

Water extracts were analyzed for pH, specific conductance (SC), dissolved organic carbon (DOC), total dissolved nitrogen (TDN), ammonia/ammonium (NH<sub>4</sub><sup>+</sup>), and nitrate/nitrite (NO<sub>x</sub><sup>-</sup>) using standard methods adopted in our previous study.<sup>24</sup> Specifically, the pH and SC were measured using an Accumet XL60 dual channel pH/ion/conductivity meter. The DOC and TDN were determined by a Shimadzu TOC/TN analyzer (SM 5310B). The NH<sub>4</sub><sup>+</sup> and NO<sub>x</sub><sup>-</sup> were measured using a Systea Easychem discrete analyzer (EPA 350.1-01 and 353.2-01). Dissolved organic nitrogen (DON) was calculated

by subtracting dissolved inorganic N ( $\text{NH}_4^+ - \text{N} + \text{NO}_x^- - \text{N}$ ) from TDN, and the DOC/DON molar ratio was calculated. The bromide concentration in water extracts was measured by ion chromatography (Dionex ICS 2100 with an AAES suppressor) using 9 mM  $\text{Na}_2\text{CO}_3$  as mobile phase. A Dionex AS-HC9 column coupled with an AG-HC9 guard column was used to separate samples. The injection volume was 250  $\mu\text{L}$ , and the minimum reporting level (MRL) was determined as 50  $\mu\text{g}/\text{L}$ .

DOM was characterized by UV-vis spectrometry (Shimadzu UV-1800) and 3D spectrofluorometry (Shimadzu Spectrofluorometer RF5301). Specific UV absorbance at 254 nm ( $\text{SUVA}_{254}$  in  $\text{L mg}^{-1} \text{m}^{-1}$ ), an indicator for aromaticity, was calculated by normalizing UV absorbance at 254 nm to DOC level.<sup>25</sup> The E2/E3 ratio, an optical index which is inversely correlated with molecular weight (MW) of DOM, was calculated as absorbance at 254 nm divided by absorbance at 365 nm.<sup>26</sup> Fluorescence excitation-emission matrices (EEMs) from 3-D spectrofluorometry were analyzed by fluorescence regional integration (FRI).<sup>27,28</sup> The fluorescence scans [excitation wavelength (Ex): 220–450 nm; emission wavelength (Em): 220–550 nm] for DOM were conducted with 5 nm slits for both excitation and emission. The raw EEM was corrected<sup>29</sup> for instrument-dependent effects, inner-filter effects, and Raman effects and standardized to Raman's units (normalized to Raman peak at Ex 350 nm). Fluorescence regional integration can be used to quantify the fluorescent DOM by dividing EEM into five operationally defined regions (I: tyrosine-like; II: tryptophan-like; III: fulvic acid-like; IV: soluble microbial byproduct-like; and V: humic acid-like).<sup>27,28</sup> The percent fluorescent response in each region ( $P_{i,n}$  for the proportion of area-normalized volume in region  $i$  to the entire region) was calculated. Several spectrofluoroscopic indices were calculated as reviewed by Fellman et al.<sup>30</sup> and references cited within. The fluorescence index (FI), an index to differentiate microbial or terrestrial origins ( $\sim 1.8$  for microbial origin and  $\sim 1.2$  for terrestrial origin), was calculated as the ratio of Em at 470 and 520 nm, at Ex 370 nm.<sup>31</sup> As  $\beta$  and  $\alpha$  peaks present the abundance of marine humic-like and terrestrial humic-like components, respectively, the freshness index ( $\beta/\alpha$ ), an index for the contribution of recently produced autochthonous DOM, was calculated as the ratio of Em at 380 nm divided by the Em maximum between 420 and 435 nm, at Ex 310 nm.<sup>32</sup> The humification index (HIX), an index of humic substance content, was determined as the area under the emission spectra 435–480 nm divided by the sum of peak areas 300–345 and 435–480 nm, at Ex 254 nm.<sup>33</sup>

**Disinfection Byproducts Formation.** In this study, we examined the formation of DBPs typically observed during chlorination and chloramination. To simulate drinking water chlorination, the DBP formation potential (FP) test was conducted on the basis of the organic and inorganic chlorine demand according to the equation  $[\text{Cl}_2] = (3 \times [\text{DOC}]) + (7.6 \times [\text{NH}_3])$ .<sup>34</sup> Briefly, all samples were diluted to a DOC concentration of 3 mg/L, buffered by  $\text{H}_3\text{BO}_3/\text{NaOH}$  solution to pH 8.0, and chlorinated with freshly prepared  $\text{NaOCl}/\text{H}_3\text{BO}_3$  solution (pH 8.0) at 25 °C in the dark for 24 h without headspace.<sup>35</sup> After reaction, the residual chlorine was quenched by 10%  $\text{Na}_2\text{SO}_3$  solution and DBPs were extracted and quantified by GC-ECD (Agilent 7890) strictly following EPA method 551.1 and EPA method 552.2.<sup>11</sup> We quantified four trihalomethanes (THMs; including trichloro-, dichlorobromo-, dibromochloro-, and tribromomethanes), five haloacetic acids

(HAAs; including chloro-, dichloro-, trichloro-, bromo-, and dibromoacetic acids), four haloacetonitriles (HANs; including trichloro-, dichloro-, bromochloro-, and dibromoacetonitriles), three halo ketones (HKs; including 1,1-dichloro-2-, 1,1,1-trichloro-2-, 1,2,3-trichloropropanones), and chloral hydrate (CHD). The MRLs for all the above DBP species were approximately 0.1–0.3  $\mu\text{g}/\text{L}$ .

*N*-Nitrosodimethylamine is the most commonly reported nitrosamine in drinking water disinfected with chloramine.<sup>36</sup> Diluted water extracts (3 mg/L DOC) were chloraminated, and NDMA was analyzed following US EPA method 521 described elsewhere.<sup>37</sup> Briefly, water extracts were reacted with excessive chloramine (100 mg/L as  $\text{Cl}_2$ ) at pH 7.8 (phosphate buffered) and stored in the dark at 22 °C for 5 days. A pH near 8 was used for both chlorination and chloramination to simulate the actual pH environment in drinking water distribution systems. After incubation, samples were quenched for residual chloramine by  $\text{Na}_2\text{SO}_3$  and extracted using solid-phase extraction employing cartridges prepaced with 2 g of coconut charcoal and eluted with dichloromethane. The extracts were analyzed using a Varian GC 3800-MS/MS 4000 equipped with a RTX-SMS column (Restek 30 m, 0.25 mm, 0.25 mm; MRL  $\sim 3$  ng/L). The detailed method is available in Note S1 in the Supporting Information.

The DOM reactivity in DBP formation was expressed as specific DBP FP ( $\mu\text{g-DBP}/\text{mg-DOC}$ ), which was calculated by dividing the DBP concentration with the initial DOC concentration. The estimated mass load of DBP precursor from the source materials, or DBP precursor yield (in  $\mu\text{g-DBP}/\text{g-detritus}$ ), was calculated by multiplying the specific DBP FP with the WEOC of the source material ( $\text{mg-DOC}/\text{g-detritus}$ ).

**Statistical Analyses.** Differences among the three sample groups (control, black ash, and white ash) were evaluated using one-way ANOVA with Tukey's HSD test. Correlations were evaluated using Pearson's correlation coefficients. Significance was considered as  $P < 0.05$ .

## RESULTS AND DISCUSSION

**General Water Quality.** The characteristics of water extracts from burned detritus (black ash or white ash;  $n = 15$ ) were distinct from nonburned detritus (control;  $n = 12$ ) (Table 1). For example, the mean pH was 6.1 for control extracts but  $> 8.5$  for ash extracts due to release of acid volatiles (e.g.,  $\text{CO}_2$ ) and deposit of alkaline residues from vegetation and organic matter by burning.<sup>38</sup> The SC of white ash extracts was higher (commonly  $> 1$  mS/cm) because much of the organic matter was burned resulting in accumulation of nonvolatile soluble inorganic elements (e.g., Ca, Mg, and K) in the ash. Burn severity significantly affected extract chemistry as reflected by consistently higher pH, SC,  $\text{NH}_4\text{-N}$ , and bromide in white ash extract than black ash extract (Tables 1 and S1, Supporting Information). Such observations agree with previous studies showing that increased burn severity (control  $\rightarrow$  black ash  $\rightarrow$  white ash) enhances volatilization and mineralization of organic matter and subsequently changes water quality of extracts.<sup>39</sup>

After fire, water extractable organic carbon (WEOC) and organic nitrogen (WEON) of the burned detritus appeared to drop significantly compared to the nonburned detritus. WEOC in detritus followed the order of  $4.31 \pm 2.66$  mg/g in control  $> 0.84 \pm 0.30$  mg/g in black ash  $\approx 0.97 \pm 0.60$  mg/g in white ash; the corresponding values for WEON were  $0.18 \pm 0.12 > 0.05 \pm 0.02 \approx 0.05 \pm 0.03$  mg/g, respectively (Figure 1). The detritus of the forest is known as an important source of

**Table 1. Characteristics of Water Extracts from Non-Burned and Burned Materials<sup>a</sup>**

parameter	control	black ash	white ash
pH	6.12 ± 1.22 <sup>c</sup>	8.57 ± 0.21 <sup>b</sup>	9.55 ± 1.25 <sup>a</sup>
specific conductance (μS/cm)	560 ± 212 <sup>b</sup>	570 ± 188 <sup>b</sup>	1195 ± 414 <sup>a</sup>
DOC (mg/L)	861 ± 531 <sup>a</sup>	168 ± 60 <sup>b</sup>	194 ± 121 <sup>b</sup>
DTN (mg/L)	43.6 ± 21.8 <sup>a</sup>	12.9 ± 4.6 <sup>b</sup>	15.4 ± 6.6 <sup>b</sup>
DON (mg/L)	35.1 ± 23.4 <sup>a</sup>	9.1 ± 3.38 <sup>b</sup>	9.51 ± 5.48 <sup>b</sup>
DOC/DON (mol/mol)	26.3 ± 6.5 <sup>a</sup>	21.9 ± 3.7 <sup>a</sup>	25.77 ± 9.9 <sup>a</sup>
NH <sub>4</sub> <sup>+</sup> -N (mg/L)	6.46 ± 2.45 <sup>a</sup>	3.51 ± 1.36 <sup>b</sup>	5.14 ± 2.32 <sup>a</sup>
NO <sub>x</sub> <sup>-</sup> -N (mg/L)	2.04 ± 1.51 <sup>a</sup>	0.35 ± 0.28 <sup>b</sup>	0.76 ± 1.46 <sup>a</sup>
Br <sup>-</sup> (μg/L)	<50 <sup>c</sup>	59 ± 20 <sup>b</sup>	131 ± 76 <sup>a</sup>
SUVA <sub>254</sub> (L/mg-C/m)	2.63 ± 0.67 <sup>a</sup>	1.77 ± 0.27 <sup>b</sup>	2.87 ± 0.8 <sup>a</sup>
E2/E3	5.80 ± 0.31 <sup>b</sup>	5.02 ± 0.89 <sup>b</sup>	9.47 ± 2.45 <sup>a</sup>
FI	1.41 ± 0.04 <sup>c</sup>	1.51 ± 0.05 <sup>b</sup>	1.63 ± 0.16 <sup>a</sup>
HIX	4.05 ± 1.48 <sup>ab</sup>	3.58 ± 0.90 <sup>b</sup>	5.54 ± 1.71 <sup>a</sup>
β/α	0.43 ± 0.03 <sup>c</sup>	0.73 ± 0.06 <sup>b</sup>	0.80 ± 0.08 <sup>a</sup>

<sup>a</sup>The letters after the mean ± standard deviation ( $n = 12$  for control;  $n = 15$  for black or white ash) refer to the significantly different groups.

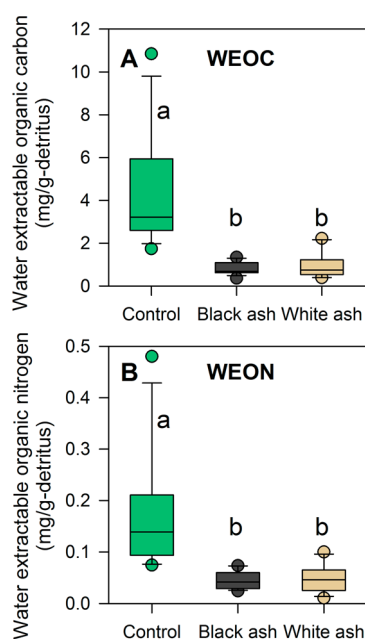


**Figure 1.** Water extractable (A) organic carbon (WEOC) and (B) organic nitrogen (WEON) from detritus/ash materials. The boxplots show the minimum, 10th, 25th, 50th, 75th, and 90th percentiles, and maximum of the data ( $n = 12$  for control;  $n = 15$  for black or white ash). Lowercase letters indicate statistically different groups.

terrestrial DOM to downstream water bodies during rainfall events.<sup>23,40</sup> However, assuming the control sites reflect the preburn conditions of the burned sites, the Rim Fire consumed much of the surficial organic materials resulting in a reduction of WEOC and WEON in leachates by 73–81% (on average), respectively.

**Characteristics of Dissolved Organic Matter.** Among the extracts, the specific UV absorbance (UV absorbance per mg-DOC) between 200 and 250 nm followed the order of white ash > control > black ash ( $P < 0.001$ ; Figure 2A and Table S3, Supporting Information), indicating that DOM from control, black ash, and white ash extracts contained different chromophoric components. Vergnoux et al.<sup>41</sup> found a higher specific UV absorbance of water extractable organic matter

(WEOM) from surface soils of recently burned sites than from control sites and attributed this to changes in the hydrophilic DOM fraction (e.g., DOM with greater  $-\text{COOH}$  moieties) rather than the hydrophobic fraction. Our results (Figure 2A) indicate that the high specific UV absorbance of WEOM is not always higher in burned sites than nonburned sites, at least not for the black ash, which usually experiences a moderate-temperature ( $\sim 200\text{--}500$  °C) pyrolysis alteration rather than high-temperature combustion/oxidation ( $>500$  °C).<sup>21</sup> Similarly, the specific UV absorbance at 254 nm (SUVA<sub>254</sub>, an aromaticity indicator of DOM) for the black ash extract ( $1.77 \pm 0.27$  L/mg-C/m) was significantly lower than the control ( $2.63 \pm 0.67$  L/mg-C/m) and white ash ( $2.87 \pm 0.80$  L/mg-C/m), suggesting that the DOM leaching from black ash was less aromatic than that from the control and white ash. Initially, it may seem surprising that black ash which commonly contains a higher content of polycondensed aromatic structures (such as polycyclic aromatic hydrocarbons; PAHs)<sup>42</sup> showed lower aromaticity in water extracts compared to the control. However, most of the condensed aromatic fraction in black ash is sparingly soluble due to the loss of  $-\text{OH}$  and/or  $-\text{COOH}$  moieties during the pyrolysis.<sup>43</sup> Consistent with SUVA<sub>254</sub> results, the humification index (HIX), a spectrofluoroscopic index that is positively linked to the degree of humification (Table 1),<sup>30</sup> suggests that the white ash extract had a higher degree of aromatic condensation than black ash extract.

The 3D fluorescence EEM also demonstrated the effects of burn severity on the DOM composition. From the overall EEM contour (Figure 2B), a significant blue shift in emission for the humic-like peaks (A peak: excitation (Ex)  $<260$  nm, Emission (Em) 448–480 nm; and C peak: Ex  $<250$  nm and 320–360 nm, Em 420–460 nm)<sup>30</sup> was observed with increasing burn severity (control → black ash → white ash), which could be attributed to a fire-induced WEOM that has more simple structures and lower molecular weight.<sup>41</sup> Besides the blue shift, both the fluorescence index (FI) and freshness index ( $\beta/\alpha$ ) (Table 1) increased with burn severity, as well as the appearance of the marine humic-like peak/shoulder (M peak: Ex  $<250$  and 290–325 nm, Em 370–430) in white ash extracts. These alterations suggest that the wildfire endows the terrestrial WEOM with similar optical properties to microbial or freshly produced autochthonous DOM that commonly has a simple structure with lower molecular weight (MW). Furthermore, the E2/E3 value is suggested as an optical index that is inversely correlated to the MW of DOM;<sup>26</sup> the higher E2/E3 values ( $P < 0.05$ ) in white ash extract (Table 1) also support the lower MW for white ash extract DOM compared to DOM from control and black ash extracts.

As burn severity increased, fluorescence regional integration showed an increased  $P_{i,n}$  in regions II and IV and a decreased response in regions I and V (Figure 2C). The decrease in region I (tyrosine-like) from  $15.1 \pm 5.6\%$  in control extracts to  $9.6 \pm 3.2\%$  in black ash extracts, and  $3.3 \pm 1.6\%$  in white ash extracts, demonstrates fire-induced protein degradation, consistent with previous molecular evidence.<sup>20</sup> The increase of region V (humic acid-like) and decrease of region IV (soluble microbial byproduct-like) suggest more simple-structured and lower-MW microbial-source-like DOM formed by the fire, consistent with results from the blue shift in emission, FI, and  $\beta/\alpha$ . In the Ex 230–250 nm/Em 340–390 nm range, an obvious peak/shoulder located in region II appeared in all white ash extracts, which we believe to be a peak related to

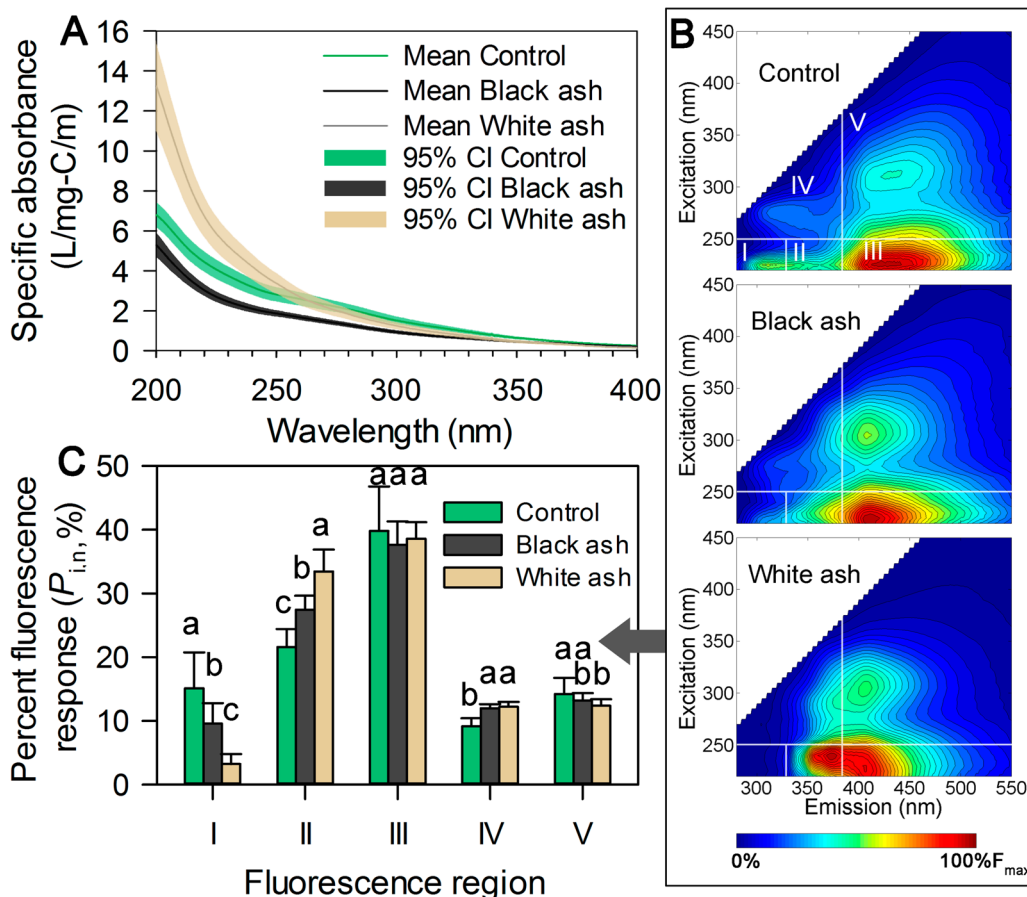


**Figure 2.** Chemical characteristics of water extractable organic matter from detritus/ash materials. (A) Specific UV absorbance (mean and 95% confidence interval (95% CI)). (B and C) 3D excitation emission matrices and fluorescence regional integration. Error bar indicates standard deviation ( $n = 12$  for control;  $n = 15$  for black or white ash), and the lowercase letters indicated statistically different groups. Roman numerals I, II, III, IV, and V are five operationally defined regions.

wildfire burn severity (WF peak) as supported by the positive correlations between percent fluorescence response in region II ( $P_{II,n}$ ) and indicators of burn severity (e.g., extract pH and SC; Figure 3A,B). Specifically,  $P_{II,n}$  increased ( $P < 0.05$ ) from 21.6

$\pm 2.8\%$  in control extracts to  $27.5 \pm 2.2\%$  in black ash extracts and  $33.5 \pm 3.4\%$  in white ash extracts (Figure 2C). This region was originally delineated as tryptophan/polyphenol-like compounds.<sup>28</sup> However, recent evidence based on Fourier transform ion cyclotron resonance mass spectrometry has shown that proteins and lignin degraded during the burning process (also supported by decreasing tyrosine-like peak in region I) and contributed to the formation of condensed aromatics.<sup>20</sup> The enhanced WF peak is therefore likely due to the increasing content of dissolved condensed aromatics rather than tryptophan-like organic matter. In fact, the fluorophore of known fire-derived polycyclic aromatic hydrocarbons (PAHs) has been previously identified at the location of the WF peak.<sup>44</sup> Therefore, we propose that the  $P_{II,n}$  of WEOM may have potential for use as a biogeochemical thermometer in fire ecology studies.

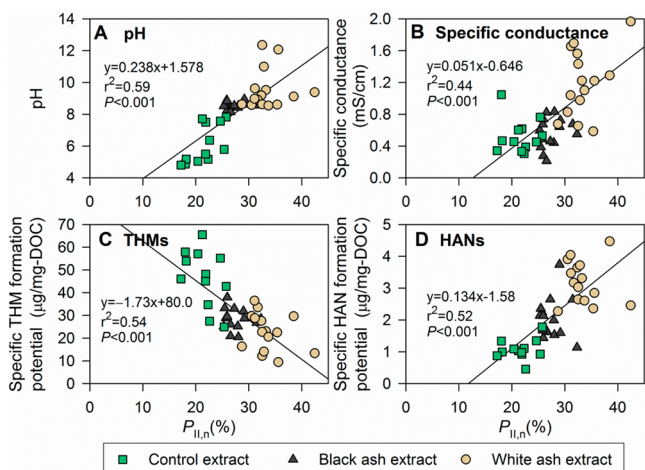


**Figure 3.** Correlations of percent fluorescent response at region II ( $P_{II,n}$ ) versus the fire-dependent properties (e.g., pH and specific conductance) and the specific disinfection byproduct formation potential [e.g., trihalomethanes (THMs) and haloacetonitriles (HANs)] ( $n = 42$ ).

**Disinfection Byproduct Formation.** After chlorination, the specific THM and specific HAA FP of the water extracts followed (Figure 4): control ( $46.6 \pm 12.5 \mu\text{g-THM}/\text{mg-DOC}$ ;  $49.1 \pm 12.8 \mu\text{g-HAA}/\text{mg-DOC}$ ) > black ash ( $28.4 \pm 4.6 \mu\text{g-THM}/\text{mg-DOC}$ ;  $38.2 \pm 9.8 \mu\text{g-HAA}/\text{mg-DOC}$ ) > white ash ( $22.7 \pm 8.3 \mu\text{g-THM}/\text{mg-DOC}$ ;  $27.6 \pm 7.4 \mu\text{g-HAA}/\text{mg-DOC}$ ) ( $P < 0.05$ ). These results indicate a reduction in the reactive THM and HAA precursors with increasing burn severity. The specific chloral hydrate (CHD) FP was  $3.0 \pm 1.0$ ,  $3.2 \pm 0.6$ , and  $3.0 \pm 0.7 \mu\text{g-CHD}/\text{mg-DOC}$  in control, black ash, and white ash extracts, respectively, and showed no

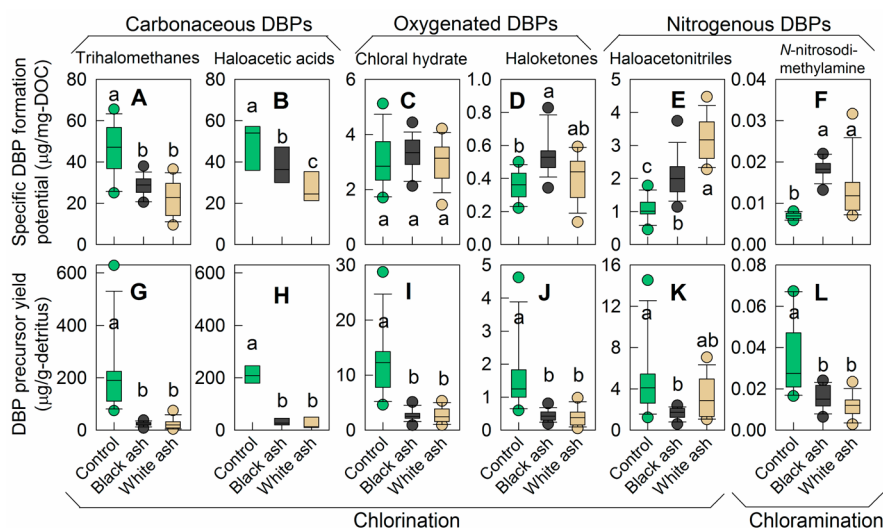


**Figure 4.** Reactivity of water extracts from detritus/ash materials in forming carbonaceous and nitrogenous disinfection byproducts (DBPs). The boxplots show the minimum, 10th, 25th, 50th, 75th, and 90th percentiles, and maximum of the data ( $n = 12$  for control;  $n = 15$  for black or white ash, except for haloacetic acid analysis which had  $n = 4$  for control and  $n = 5$  for both ashes). Lowercase letters indicate statistically different groups.

dependence on burn severity (Figure 4). For halo ketones (HKs), the black ash extract had a higher specific FP of  $0.54 \pm 0.12 \mu\text{g-HK/mg-DOC}$  compared to the control ( $0.36 \pm 0.09 \mu\text{g-HK/mg-DOC}$ ) and white ash extracts ( $0.40 \pm 0.14 \mu\text{g-HK/mg-DOC}$ ). In contrast to THMs and HAAs, the more toxic nitrogenous DBPs, HANs, showed a significant increase in specific FP with increasing burn severity: control extract ( $1.07 \pm 0.32 \mu\text{g-HAN/mg-DOC}$  or  $26.2 \pm 5.9 \mu\text{g-HAN/mg-DON}$ ) < black ash ( $2.04 \pm 0.65 \mu\text{g-HAN/mg-DOC}$  or  $38.2 \pm 13.7 \mu\text{g-HAN/mg-DON}$ ) < white ash ( $3.2 \pm 0.67 \mu\text{g-HAN/mg-DOC}$  or  $67.8 \pm 20.9 \mu\text{g-HAN/mg-DON}$ ). After chloramination, the specific NDMA FP was significantly higher in ash extracts (black ash:  $18.3 \pm 2.4 \text{ ng-NDMA/mg-DOC}$  or  $344 \pm 72 \mu\text{g-NDMA/mg-DON}$ ; white ash:  $13.5 \pm 6.5 \text{ ng-NDMA/mg-DOC}$  or  $270 \pm 90 \mu\text{g-NDMA/mg-DON}$ ) than in control extracts ( $6.9 \pm 0.7 \text{ ng-NDMA/mg-DOC}$  or  $176 \pm 37 \mu\text{g-NDMA/mg-DON}$ ).

The specific DBP FP is closely linked to the composition of organic matter, i.e., the relative abundance of reactive components in organic matter.<sup>45</sup> Before burning, the detritus contained a substantial amount of biopolymers, such as lignin and protein. The lignin phenols and aromatic moieties of proteins are both known to be highly reactive THM and HAA precursors,<sup>45,46</sup> e.g., up to  $328 \mu\text{g-THM/mg-C}$  for acetosyringone and  $138 \mu\text{g-THM/mg-C}$  for tyrosine. The fire consumes many of these precursors and transforms them to condensed aromatics (such as PAHs).<sup>47</sup> These condensed aromatics, which can account for more than half of the DOM structure in the extract, impart the DOM with lower H/C and O/C ratios and a much higher double bond equivalent.<sup>47,48</sup> The ash extracts possessed lower reactivity in forming THM and HAA suggesting that the condensed aromatics were likely less reactive THM and HAA precursors. Although high specific THM and HAA FP often positively link to high DOM aromaticity (or high  $\text{SUVA}_{254}$ ),<sup>49</sup>  $\text{SUVA}_{254}$  could not explain the DOM reactivity in THM or HAA formation across the three DOM sources in this study ( $r^2 = 0.06$ ,  $P = 0.12\text{--}0.19$ ; Figure S3, Supporting Information). Compared to  $\text{SUVA}_{254}$ ,  $P_{\text{II},n}$  demonstrated stronger linear correlations with specific THM and HAA FP ( $r^2 = 0.54$  for THM,  $r^2 = 0.72$  for HAA;  $P <$

0.001; Figure 3C shows THM), suggesting that DOM reactivity in forming THM and HAA decreased with increasing burn severity. This may be because the chlorination of condensed aromatics, compared to the chlorination of plant-derived phenolics, requires higher energy to break down double bond structures to generate the simple aliphatic THM or HAA structures. Some chlorinated PAHs have been found as alternative reaction products from chlorination of condensed-aromatics (PAH-) spiked natural waters,<sup>50</sup> suggesting the possibility for formation of other chlorinated products other than THMs or HAAs.

Despite findings that specific HAN FP increases with a decreasing C/N ratio of the original organic matter during the humification process,<sup>45</sup> the enhanced specific HAN and NDMA FP with increasing burn severity cannot be simply explained by DON, TDN, DOC/TDN, or DOC/DON patterns ( $P > 0.05$ ; Table 1). The change of organic nitrogen structure with increasing burn severity is probably the major factor because specific HAN FP linearly increased with  $P_{\text{II},n}$  ( $r^2 = 0.52$ ,  $P < 0.001$ ; Figure 3D) and decreased with  $P_{\text{I},n}$  (protein-like compound;  $r^2 = 0.59$ ,  $P < 0.001$ ; Figure S4, Supporting Information). While most of the organic nitrogen in nonburned detritus was dominated by amide/peptide forms, the fire process leads to polymerization of N and generates heteroaromatic N as a major form of organic N.<sup>20</sup> The formation of dissolved black nitrogen compounds from polymerization of N into the condensed aromatic structure is probably a major reason for enhanced reactivity of HAN formation. NDMA, however, did not show this same linear correlation with  $P_{\text{II},n}$ , but rather a bell-shaped relationship with  $P_{\text{II},n}$ . This suggests that NDMA and HAN precursors were different, and the reactive NDMA precursors were formed at moderate burning temperatures (200–500 °C) but subsequently degraded when the temperature reached higher levels (>510 °C) in severe burning. Our results of enhanced reactivity in forming HANs of fire-affected terrestrial DOM can well explain the enhanced HAN formation in water samples from burned watersheds.<sup>7</sup> Here, we found that the fire-altered terrestrial DOM was at the high end of natural organic matter in reactivity for N-DBP formation. In spite of a relatively high

DOC/DON ratio ( $\sim 16\text{--}36$ ), this DOM was more reactive than humic acids (commonly  $<2 \mu\text{g-HAN/mg-C}$  and  $\text{DOC/DON} >10$ ) and even nitrogen-rich natural organic matter sources such as algal and bacterial materials (commonly  $\sim 2\text{--}3 \mu\text{g-HAN/mg-C}$  and  $\text{C/N}$  of  $3\text{--}6$ ).<sup>11,51,52</sup> Given the ubiquitous presence of dissolved black nitrogen in freshwater DOM,<sup>53</sup> the hitherto unidentified fire-altered fraction in DOM may disproportionately contribute to the watershed budget of N-DBP precursors following wildfire.

Although DBP FP tests are conducted using excess chlorine to determine the overall precursor amount in a sample which favors the formation of chlorinated THM and HAA species, the results showed that the fire process significantly enhanced the brominated DBP fraction compared to nonburned detritus (bromine incorporation factor: control =  $0.04 \pm 0.01\%$ , black ash =  $0.39 \pm 0.22\%$ , and white ash =  $1.6 \pm 1.0\%$ ; Figure 5). The

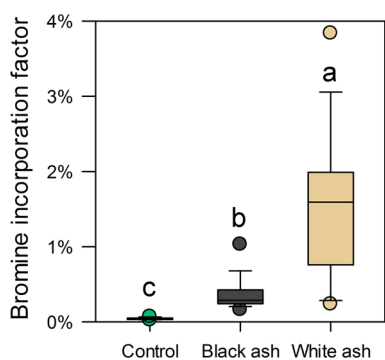


**Figure 5.** Bromine incorporation factor of trihalomethanes formed from chlorination of dissolved organic matter from burned and nonburned detritus/ash extracts. The boxplots show the minimum, 10th, 25th, 50th, 75th, and 90th percentiles, and maximum of the data. Lowercase letters indicate statistically different groups.

major factor contributing higher brominated DBPs was the accumulation of inorganic bromide in the ash following its release from organic materials by combustion (Table 1). Bromide reacts with chlorine to generate reactive bromine species which can be incorporated into brominated DBPs.<sup>54</sup>

The DBP precursor yield of the terrestrial detritus depends on both the reactivity (i.e., quality) and the quantity of WEOM. Although the reactivity for DBP formation either increased or decreased with burn severity depending on the specific DBP species, the difference in WEOM quantity among samples was more significant and overwhelmed differences in specific DBP FP (Figure 1). Assuming the control sites reflect the preburn conditions of the burned sites, the control to black ash transformation resulted in decreased DBP precursor yields: 88.6% THMs, 85.0% HAAs, 78.1% CHD, 71.8% HKs, 66.0% HANs, and 51.7% NDMA (Figure 4G–L). DBP precursor yield showed a similar decrease from control to white ash samples with the exception of HANs being considerably reduced relative to black ash: 88.4% THMs, 87.4% HAAs, 77.9% CHD, 74.9% HKs, 34.6% HANs, and 65.7% NDMA (Figure 4G–L).

**Implications and Perspectives.** Currently, one major difficulty in understanding the net effects of wildfire on DOM quality and quantity in natural waters is that interference from background watershed sources of DOM may overwhelm the effects of fire, especially when a low percentage of the watershed is burned.<sup>7</sup> The hydrological, topographical, physicochemical, and microbiological processes for DOM

leaching from soil to stream can also significantly affect DOM chemistry.<sup>55,56</sup> Evaluating terrestrial DBP precursors from fire-affected WEOM is an important first step to elucidate the direct effects of fire on watershed DBP precursors. Using water extracts from detritus materials instead of stream waters, we demonstrated that the effects of wildfire on the reactivity of terrestrial DOM in DBP formation were not uniform, with lower reactivity for carbonaceous DBPs such as THMs and HAAs but higher reactivity for more toxic nitrogenous DBPs such as HANs and NDMA. By implication, when the first postfire rainfall/storm event brings fire-affected terrestrial DOM into the source water, attention should be placed on the formation of nitrogenous DBPs in addition to carbonaceous DBPs during water treatment.

Although wildfire is often associated with downstream water quality degradation from substances such as sediment, nutrients, heavy metals, and organic pollutants,<sup>2,5</sup> the results of our study (Figure 4G–L) indicated that the estimated terrestrial mass load of DBP precursors from detritus materials in burned forests can be reduced in the short term compared to nonburned forests for the major DBP classes. This was mainly due to the large loss of organic matter by the fire. It should be noted that the mass load estimation of DBP precursors was based on the same extraction conditions for nonburned and burned detritus in the lab. Under field conditions for a specific forest wildfire event, environmental factors, such as microclimate, sunlight exposure, water temperature, soil–water residence time, fire-induced soil/sediment erosion, and altered hydrological flows in the burned watershed,<sup>5,7</sup> will likely affect the quality and quantity of DBP precursors leaching from terrestrial sources in a single rainfall event, resulting in potentially altered results. Importantly, a couple of studies<sup>2,57</sup> have found that the stream DOC levels could be enhanced postfire due to a large degree of soil erosion, which may pose enhanced threats of DBP formation. Although we have demonstrated the effects of wildfires on terrestrial DBP precursors, the current knowledge on increasing frequency and severity of forest fires on drinking water quality and associated human health is still in its infancy. Future research on this topic can help to elucidate the relevant environmental processes and consequences and reveal linkages among forest disturbance, water quality, human health, and climate change.

## ■ ASSOCIATED CONTENT

### 📄 Supporting Information

Detailed methods for *N*-nitrosodimethylamine (NDMA) analysis, Tables S1–S6, Figures S1–S4. The Supporting Information is available free of charge on the ACS Publications website at DOI: 10.1021/es505836m.

## ■ AUTHOR INFORMATION

### Corresponding Author

\*E-mail: achow@clemson.edu; tel: +1 843 546 1013 x232; fax: +1 843 546 6296.

### Notes

The authors declare no competing financial interest.

## ■ ACKNOWLEDGMENTS

This work was funded by an NSF RAPID grant (1264579) and partially supported by NIFA/USDA (SC1700489 and 2014-67019-21615) and Joint Fire Science Program (14-1-06-19), as presented in technical contribution number 6361 of the

Clemson University Experiment Station. J.W. appreciates financial support from the China Scholarship Council (CSC [2011]3010). We thank the U.S. Forest Service for the access to sample collection in Rim Fire-affected area. The authors acknowledge associate editor Dr. Richard L. Valentine and four anonymous reviewers for their valuable comments that significantly improve this paper.

## REFERENCES

- (1) United States Forest Service (USFS) *The U.S. Forest Service - An Overview*; 2007; [http://www.fs.fed.us/documents/USFS\\_An\\_Overview\\_0106MJS.pdf](http://www.fs.fed.us/documents/USFS_An_Overview_0106MJS.pdf) (Assessed on Oct. 2, 2014).
- (2) Bladon, K. D.; Emelko, M. B.; Silins, U.; Stone, M. Wildfire and the future of water supply. *Environ. Sci. Technol.* **2014**, *48* (16), 8936–8943.
- (3) Westerling, A. L.; Hidalgo, H. G.; Cayan, D. R.; Swetnam, T. W. Warming and earlier spring increase western US forest wildfire activity. *Science* **2006**, *313* (5789), 940–943.
- (4) Rhoades, C. C.; Entwistle, D.; Butler, D. The influence of wildfire extent and severity on streamwater chemistry, sediment and temperature following the Hayman Fire, Colorado. *Int. J. Wildland Fire* **2011**, *20* (3), 430–442.
- (5) Smith, H. G.; Sheridan, G. J.; Lane, P. N. J.; Nyman, P.; Haydon, S. Wildfire effects on water quality in forest catchments: A review with implications for water supply. *J. Hydrol.* **2011**, *396* (1–2), 170–192.
- (6) Emelko, M. B.; Silins, U.; Bladon, K. D.; Stone, M. Implications of land disturbance on drinking water treatability in a changing climate: Demonstrating the need for “source water supply and protection” strategies. *Water Res.* **2011**, *45* (2), 461–472.
- (7) Writer, J. H.; Hohner, A.; Oropeza, J.; Schmidt, A.; Cawley, K. M.; Rosario-Ortiz, F. L. Water treatment implications after the High Park Wildfire, Colorado. *J. Am. Water Works Assoc.* **2014**, *106* (4), E189–E199.
- (8) Sedlak, D. L.; von Gunten, U. The chlorine dilemma. *Science* **2011**, *331* (6013), 42–43.
- (9) Karanfil, T.; Krasner, S. W.; Westerhoff, P.; Xie, Y. F. *Disinfection by-products in drinking water: Occurrence, formation, health effects, and control*; Oxford University Press: Washington, DC, USA, 2008.
- (10) Krasner, S. W.; Mitch, W. A.; McCurry, D. L.; Hanigan, D.; Westerhoff, P. Formation, precursors, control, and occurrence of nitrosamines in drinking water: A review. *Water Res.* **2013**, *47* (13), 4433–4450.
- (11) Wang, J. J.; Liu, X.; Ng, T. W.; Xiao, J. W.; Chow, A. T.; Wong, P. K. Disinfection byproduct formation from chlorination of pure bacterial cells and pipeline biofilms. *Water Res.* **2013**, *47* (8), 2701–2709.
- (12) Deborde, M.; von Gunten, U. Reactions of chlorine with inorganic and organic compounds during water treatment - kinetics and mechanisms: A critical review. *Water Res.* **2008**, *42* (1–2), 13–51.
- (13) Hrudey, S. E. Chlorination disinfection by-products, public health risk tradeoffs and me. *Water Res.* **2009**, *43* (8), 2057–2092.
- (14) Richardson, S. D.; Plewa, M. J.; Wagner, E. D.; Schoeny, R.; DeMarini, D. M. Occurrence, genotoxicity, and carcinogenicity of regulated and emerging disinfection by-products in drinking water: A review and roadmap for research. *Mutat. Res., Rev. Mutat. Res.* **2007**, *636* (1–3), 178–242.
- (15) Plewa, M. J.; Wagner, E. D. *Mammalian cell cytotoxicity and genotoxicity of disinfection by-products*; Water Research Foundation: Denver, CO, USA, 2009.
- (16) Rhoades, C. C.; McCutchan, J. H.; Cooper, L. A.; Clow, D.; Detmer, T. M.; Briggs, J. S.; Stednick, J. D.; Veblen, T. T.; Ertz, R. M.; Likens, G. E.; Lewis, W. M. Biogeochemistry of beetle-killed forests: Explaining a weak nitrate response. *Proc. Natl. Acad. Sci. U.S.A.* **2013**, *110* (5), 1756–1760.
- (17) Mikkelsen, K. M.; Dickenson, E. R. V.; Maxwell, R. M.; McCray, J. E.; Sharp, J. O. Water-quality impacts from climate-induced forest die-off. *Nat. Clim. Change* **2013**, *3* (3), 218–222.
- (18) Bowman, D. M. J. S.; Balch, J. K.; Artaxo, P.; Bond, W. J.; Carlson, J. M.; Cochrane, M. A.; D’Antonio, C. M.; DeFries, R. S.; Doyle, J. C.; Harrison, S. P.; Johnston, F. H.; Keeley, J. E.; Krawchuk, M. A.; Kull, C. A.; Marston, J. B.; Moritz, M. A.; Prentice, I. C.; Roos, C. I.; Scott, A. C.; Swetnam, T. W.; van der Werf, G. R.; Pyne, S. J. Fire in the earth system. *Science* **2009**, *324* (5926), 481–484.
- (19) Dittmar, T.; de Rezende, C. E.; Manecki, M.; Niggemann, J.; Ovalle, A. R. C.; Stubbins, A.; Bernardes, M. C. Continuous flux of dissolved black carbon from a vanished tropical forest biome. *Nat. Geosci.* **2012**, *5* (9), 618–622.
- (20) Knicker, H. How does fire affect the nature and stability of soil organic nitrogen and carbon? A review. *Biogeochemistry* **2007**, *85* (1), 91–118.
- (21) Bodi, M. B.; Martin, D. A.; Balfour, V. N.; Santin, C.; Doerr, S. H.; Pereira, P.; Cerda, A.; Mataix-Solera, J. Wild land fire ash: Production, composition and eco-hydro-geomorphic effects. *Earth-Sci. Rev.* **2014**, *130*, 103–127.
- (22) Cilimburg, A. C.; Short, K. C. Rating the severity of fire in forest soils. In *Forest fire in the U. S. Northern Rockies: A primer*; 2005; <http://www.northernrockiesfire.org/effects/soilrate.htm> (Assessed on Oct. 2, 2014).
- (23) Chow, A. T.; Lee, S. T.; O’Geen, A. T.; Orozco, T.; Beaudette, D.; Wong, P. K.; Hernes, P. J.; Tate, K. W.; Dahlgren, R. A. Litter contributions to dissolved organic matter and disinfection byproduct precursors in California oak woodland watersheds. *J. Environ. Qual.* **2009**, *38* (6), 2334–2343.
- (24) Chow, A. T.; Dai, J. N.; Conner, W. H.; Hitchcock, D. R.; Wang, J. J. Dissolved organic matter and nutrient dynamics of a coastal freshwater forested wetland in Winyah Bay, South Carolina. *Biogeochemistry* **2013**, *112* (1–3), 571–587.
- (25) Karanfil, T.; Schlautman, M. A.; Erdogan, I. Survey of DOC and UV measurement practices with implications for SUVA determination. *J. Am. Water Works Assoc.* **2002**, *94* (12), 68–80.
- (26) Peuravuori, J.; Pihlaja, K. Molecular size distribution and spectroscopic properties of aquatic humic substances. *Anal. Chim. Acta* **1997**, *337* (2), 133–149.
- (27) Zhou, J.; Wang, J. J.; Baudon, A.; Chow, A. T. Improved fluorescence excitation-emission matrix regional integration to quantify spectra for fluorescent dissolved organic matter. *J. Environ. Qual.* **2013**, *42* (3), 925–930.
- (28) Chen, W.; Westerhoff, P.; Leenheer, J. A.; Booksh, K. Fluorescence excitation-emission matrix regional integration to quantify spectra for dissolved organic matter. *Environ. Sci. Technol.* **2003**, *37* (24), 5701–5710.
- (29) Murphy, K. R.; Butler, K. D.; Spencer, R. G. M.; Stedmon, C. A.; Boehme, J. R.; Aiken, G. R. Measurement of dissolved organic matter fluorescence in aquatic environments: An interlaboratory comparison. *Environ. Sci. Technol.* **2010**, *44* (24), 9405–9412.
- (30) Fellman, J. B.; Hood, E.; Spencer, R. G. M. Fluorescence spectroscopy opens new windows into dissolved organic matter dynamics in freshwater ecosystems: A review. *Limnol. Oceanogr.* **2010**, *55* (6), 2452–2462.
- (31) Cory, R. M.; McKnight, D. M. Fluorescence spectroscopy reveals ubiquitous presence of oxidized and reduced quinones in dissolved organic matter. *Environ. Sci. Technol.* **2005**, *39* (21), 8142–8149.
- (32) Wilson, H. F.; Xenopoulos, M. A. Effects of agricultural land use on the composition of fluvial dissolved organic matter. *Nat. Geosci.* **2009**, *2* (1), 37–41.
- (33) Ohno, T. Fluorescence inner-filtering correction for determining the humification index of dissolved organic matter. *Environ. Sci. Technol.* **2002**, *36* (4), 742–746.
- (34) Krasner, S.; Sclementi, M. Characterization of natural organic matter: Disinfection by-product analysis. In *Workshop on Natural Organic Matter in Drinking Water: Origin, Characterization, and Removal, Proceedings*, Denver, CO, USA, 1993; p 9.
- (35) Summers, R. S.; Hooper, S. M.; Shukairy, H. M.; Solarik, G.; Owen, D. Assessing the DBP yield: Uniform formation conditions. *J. Am. Water Works Assoc.* **1996**, *88* (6), 80–93.



- (36) Shah, A. D.; Mitch, W. A. Halonitroalkanes, halonitriles, haloamides, and *N*-nitrosamines: A critical review of nitrogenous disinfection byproduct formation pathways. *Environ. Sci. Technol.* **2012**, *46* (1), 119–131.
- (37) Selbes, M.; Kim, D.; Ates, N.; Karanfil, T. The roles of tertiary amine structure, background organic matter and chloramine species on NDMA formation. *Water Res.* **2013**, *47* (2), 945–953.
- (38) Certini, G. Effects of fire on properties of forest soils: A review. *Oecologia* **2005**, *143* (1), 1–10.
- (39) Goforth, B. R.; Graham, R. C.; Hubbert, K. R.; Zanner, C. W.; Minnich, R. A. Spatial distribution and properties of ash and thermally altered soils after high-severity forest fire, southern California. *Int. J. Wildland Fire* **2005**, *14* (4), 343–354.
- (40) Dosskey, M. G.; Bertsch, P. M. Forest sources and pathways of organic-matter transport to a blackwater stream - A hydrologic approach. *Biogeochemistry* **1994**, *24* (1), 1–19.
- (41) Vergnoux, A.; Di Rocco, R.; Domeizel, M.; Guiliano, M.; Doumenq, P.; Theraulaz, F. Effects of forest fires on water extractable organic matter and humic substances from Mediterranean soils: UV-vis and fluorescence spectroscopy approaches. *Geoderma* **2011**, *160* (3–4), 434–443.
- (42) Preston, C. M.; Schmidt, M. W. I. Black (pyrogenic) carbon: A synthesis of current knowledge and uncertainties with special consideration of boreal regions. *Biogeosciences* **2006**, *3* (4), 397–420.
- (43) Schnitzer, M.; Hoffman, I. Pyrolysis of soil organic matter. *Soil Sci. Soc. Am. J.* **1964**, *28* (4), 520–525.
- (44) Rudnick, S. M.; Chen, R. F. Laser-induced fluorescence of pyrene and other polycyclic aromatic hydrocarbons (PAH) in seawater. *Talanta* **1998**, *47* (4), 907–919.
- (45) Wang, J. J.; Ng, T. W.; Zhang, Q.; Yang, X. B.; Dahlgren, R. A.; Chow, A. T.; Wong, P. K. Technical Note: Reactivity of C1 and C2 organohalogen formation – from plant litter to bacteria. *Biogeosciences* **2012**, *9* (10), 3721–3727.
- (46) Hua, G. H.; Kim, J.; Reckhow, D. A. Disinfection byproduct formation from lignin precursors. *Water Res.* **2014**, *63*, 285–295.
- (47) Podgorski, D. C.; Hamdan, R.; McKenna, A. M.; Nyadong, L.; Rodgers, R. P.; Marshall, A. G.; Cooper, W. T. Characterization of pyrogenic black carbon by desorption atmospheric pressure photo-ionization Fourier transform ion cyclotron resonance mass spectrometry. *Anal. Chem.* **2012**, *84* (3), 1281–1287.
- (48) Ward, C. P.; Sleighter, R. L.; Hatcher, P. G.; Cory, R. M. Insights into the complete and partial photooxidation of black carbon in surface waters. *Environ. Sci.: Processes Impacts* **2014**, *16* (4), 721–731.
- (49) Chow, A. T.; Dahlgren, R. A.; Zhang, Q.; Wong, P. K. Relationships between specific ultraviolet absorbance and trihalomethane precursors of different carbon sources. *J. Water Supply: Res. Technol.* **2008**, *57* (7), 471–480.
- (50) Johnsen, S.; Gribbestad, I. S.; Johansen, S. Formation of chlorinated PAH - A possible health-hazard from water chlorination. *Sci. Total Environ.* **1989**, *81–2*, 231–238.
- (51) Fang, J. Y.; Ma, J.; Yang, X.; Shang, C. Formation of carbonaceous and nitrogenous disinfection by-products from the chlorination of *Microcystis aeruginosa*. *Water Res.* **2010**, *44* (6), 1934–1940.
- (52) Lee, W.; Westerhoff, P.; Croue, J. P. Dissolved organic nitrogen as a precursor for chloroform, dichloroacetonitrile, *N*-nitrosodimethylamine, and trichloronitromethane. *Environ. Sci. Technol.* **2007**, *41* (15), 5485–5490.
- (53) Ding, Y.; Watanabe, A.; Jaffé, R. Dissolved black nitrogen (DBN) in freshwater environments. *Org. Geochem.* **2014**, *68*, 1–4.
- (54) Heeb, M. B.; Criquet, J.; Zimmermann-Steffens, S. G.; von Gunten, U. Oxidative treatment of bromide-containing waters: Formation of bromine and its reactions with inorganic and organic compounds - A critical review. *Water Res.* **2014**, *48*, 15–42.
- (55) Pacific, V. J.; Jencso, K. G.; McGlynn, B. L. Variable flushing mechanisms and landscape structure control stream DOC export during snowmelt in a set of nested catchments. *Biogeochemistry* **2010**, *99* (1–3), 193–211.
- (56) McGlynn, B. L.; McDonnell, J. J. Role of discrete landscape units in controlling catchment dissolved organic carbon dynamics. *Water Resour. Res.* **2003**, *39* (4), 1–17.
- (57) Revchuk, A. D.; Suffet, I. H. Effect of wildfires on physicochemical changes of watershed dissolved organic matter. *Water Environ. Res.* **2014**, *86*, 372–381.